



Contents lists available at ScienceDirect

## Journal of Non-Crystalline Solids

journal homepage: [www.elsevier.com/locate/jnoncrysol](http://www.elsevier.com/locate/jnoncrysol)

Letter to the Editor

Thermal stability of amorphous  $Mg_{50}Ni_{50}$  alloy produced by mechanical alloyingD. Guzmán<sup>a,\*</sup>, S. Ordoñez<sup>b</sup>, D. Serafini<sup>c</sup>, P.A. Rojas<sup>d</sup>, C. Aguilar<sup>e</sup>, M. Santander<sup>a</sup><sup>a</sup>Departamento de Ingeniería en Metalurgia, Facultad de Ingeniería, Universidad de Atacama y Centro Regional de Investigación y Desarrollo Sustentable de Atacama, Av. Copayapu 485, Copiapó, Chile<sup>b</sup>Departamento de Ingeniería Metalúrgica, Facultad de Ingeniería, Universidad de Santiago de Chile, Av. Lib. Bernardo O'Higgins 3363, Santiago, Chile<sup>c</sup>Departamento de Física, Facultad de Ciencias, Universidad de Santiago de Chile and Center for Interdisciplinary Research in Materials, CIMAT, Av. Lib. Bernardo O'Higgins 3363, Santiago, Chile<sup>d</sup>Escuela de Ingeniería Mecánica, Facultad de Ingeniería, Av. Los Carrera 01567, Quilpué, Pontificia Universidad Católica de Valparaíso, PUCV, Chile<sup>e</sup>Instituto de Materiales y Procesos Termomecánicos, Facultad de Ciencias de la Ingeniería, Universidad Austral de Chile, Av. General Lagos 2086, Valdivia, Chile

## ARTICLE INFO

## Article history:

Received 7 February 2009

Received in revised form 24 September 2009

Available online 20 November 2009

## Keywords:

Amorphous metals, metallic glasses

Alloys

Mechanical alloying

X-ray diffraction

Powders

Thermal properties

## ABSTRACT

Amorphous  $Mg_{50}Ni_{50}$  alloy was produced by mechanical alloying (MA) of the elemental powders Mg and Ni using a SPEX 8000D mill. The alloyed powders were microstructurally characterized by X-ray diffraction (XRD). The thermal transformation of amorphous  $Mg_{50}Ni_{50}$  into stable intermetallics ( $Mg_{50}Ni_{50} \rightarrow$  remaining amorphous +  $Mg_2Ni \rightarrow Mg_2Ni + MgNi_2$ ) was analyzed using the Kissinger and isoconversional methods based on the non-isothermal differential scanning calorimetry (DSC) experiments. The apparent activation energies ( $E_a$ ) and the transformation diagrams, temperature–time–transformation ( $T$ – $T$ – $T$ ) and temperature–heating rate–transformation ( $T$ – $HR$ – $T$ ), were obtained for both processes. A good agreement was observed between the calculated transformation curves and the experimental data, which verifies the reliability of the method utilized.

© 2009 Elsevier B.V. All rights reserved.

## 1. Introduction

The knowledge of thermal behavior of materials is important in controlling their structure and properties. Several authors have proposed some mathematical models in order to calculate the amount of transformed material during crystallization [1–3]. This development has led to the determination of  $T$ – $T$ – $T$  and  $T$ – $HR$ – $T$  diagrams for the description of the amorphous crystallization process [4–6].

On the other hand, amorphous  $Mg_{50}Ni_{50}$ , produced by MA, has shown a marked improvement in the hydriding–dehydriding kinetics compared to  $Mg_2Ni$  and ball-milled  $Mg_2Ni$  [7,8]. To maintain the improved hydrogen storage properties upon cycling, the thermal stability of amorphous structures must be considered. In the present work, the thermal transformation of amorphous  $Mg_{50}Ni_{50}$  into stable intermetallics ( $Mg_{50}Ni_{50} \rightarrow$  remaining amorphous +  $Mg_2Ni \rightarrow Mg_2Ni + MgNi_2$ ) has been studied using the Kissinger [9] and isoconversional methods [10,11]. Furthermore,  $T$ – $T$ – $T$  and  $T$ – $HR$ – $T$  diagrams have been obtained for both reactions using the procedure developed by Suñol et al. [12].

## 2. Experimental procedure

Amorphous  $Mg_{50}Ni_{50}$  was produced by MA of Mg turnings (98 wt% pure, supplied by Aldrich) and Ni powder (99.99 wt% pure, supplied by Fluka) in a 1:1 atomic proportion, in a high-energy SPEX 8000D mill, with a ball to powder weight ratio of 20:1 under controlled atmosphere of Ar. XRD measurements were carried out in a Shimadzu XRD-600 diffractometer with  $Cu K\alpha$  radiation. The internal microstructure of the powder was studied using a FEI Tecnai G2 F20 S-Twin transmission electron microscope (TEM). Thermal stability was determined by means of non-isothermal DSC experiments under  $N_2$  flowing in a SDT 2960 (TA instruments) device. The heating rates ranged from 10 to 40 K/min.

## 3. Results

Typical examples of high-resolution electron micrograph and selection area diffraction from the amorphous  $Mg_{50}Ni_{50}$  alloy are shown in Fig 1. It can be observed that the milled material is not fully amorphous. It is constituted by two contributions: nanocrystalline (crystallite size  $\leq 5$  nm) and amorphous phase. The electron diffraction pattern indexation was very complicated due to the diffused diffraction rings. The possible crystalline phases present in

\* Corresponding author. Tel.: +56 52 206646.

E-mail address: [danny.guzman@uda.cl](mailto:danny.guzman@uda.cl) (D. Guzmán).

the milled powder could be  $\text{Mg}_2\text{Ni}$ ,  $\text{MgNi}_2$  and  $\text{Ni}$ . A detailed study of the phase evolution during the amorphization process can be found in reference [13].

Fig. 2 shows the DSC traces of amorphous  $\text{Mg}_{50}\text{Ni}_{50}$  alloy using several heating rates. The calorimetry scans show the presence of three exothermic events. According to a previous investigation [14,15], the first broad peak situated around 400 K is the result of the structural relaxation of the amorphous structure, while the second and third peaks correspond to the transformation of amorphous phase into nanocrystalline  $\text{Mg}_2\text{Ni}$  and  $\text{MgNi}_2$ , respectively.

Depending on the heating rate employed, the first transformation reaction ( $\text{Mg}_{50}\text{Ni}_{50} \rightarrow \text{Mg}_2\text{Ni} + \text{remaining amorphous}$ ) takes

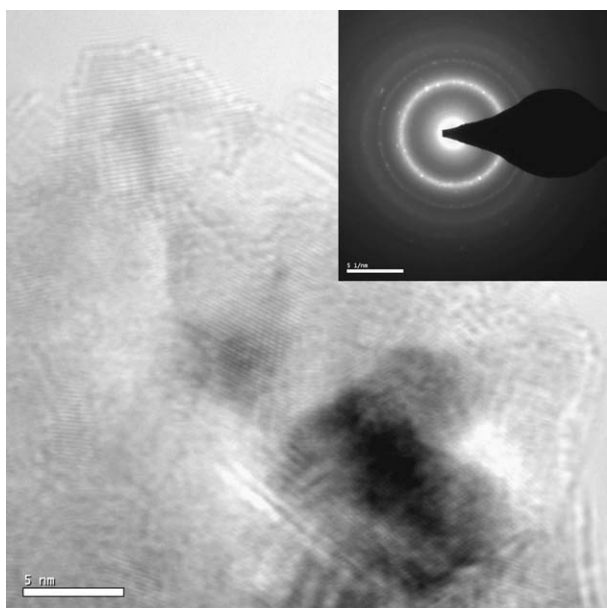


Fig. 1. High-resolution electron micrograph and selection area diffraction of amorphous  $\text{Mg}_{50}\text{Ni}_{50}$ .

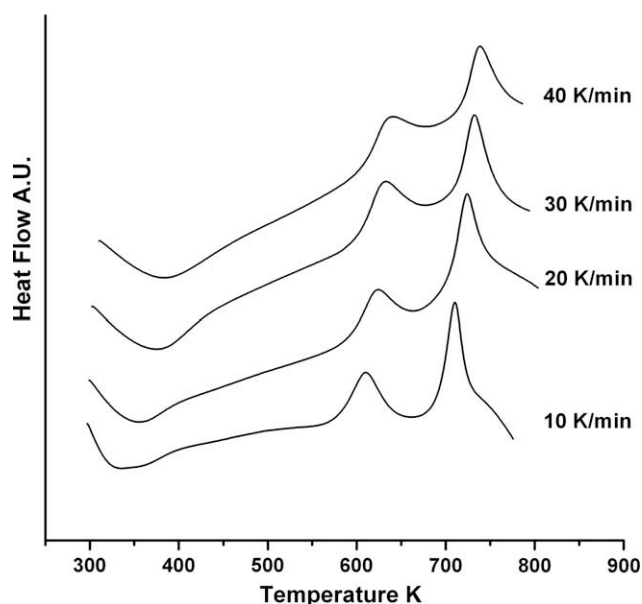


Fig. 2. DSC traces recorded at different heating rates (10, 20, 30 and 40 K/min) for the thermal transformation of  $\text{Mg}_{50}\text{Ni}_{50}$  amorphous alloy into stable intermetallics.

place between 610 and 641 K, whereas the second ( $\text{Mg}_2\text{Ni} + \text{remaining amorphous} \rightarrow \text{Mg}_2\text{Ni} + \text{MgNi}_2$ ) takes place between 710 and 739 K. The peak temperatures obtained are close to those reported in previous works [14,15].

The activation energies for the transformation processes were estimated by the Kissinger [9] and isoconversional methods [10,11]. The activation energies calculated by Kissinger method obtained for both transformation reactions were  $135 \pm 4 \text{ kJ mol}^{-1}$  and  $200 \pm 2 \text{ kJ mol}^{-1}$ , respectively.

To obtain the activation energies by isoconversional method, experimental data were analyzed in the range of transformed fraction ( $\alpha$ ) from 0.1 to 0.9 to avoid the deviation due to experimental errors for very high and low values of  $\alpha$  [16]. The activation energy obtained for first reaction was  $142 \pm 9 \text{ kJ mol}^{-1}$  (Fig. 3(a)), whereas the activation energy obtained for the second transformation reaction was not constant with  $\alpha$  (Fig. 3(b)). It is possible to observe three zones:

$$E_a(\alpha) \text{ kJ mol}^{-1} = \begin{cases} 170 \pm 5 & [0.1 - 0.3] \\ (221 \pm 3) - (170 \pm 6)\alpha & [0.3 - 0.6] \\ 111 \pm 9 & [0.6 - 0.9] \end{cases} \quad (1)$$

Fig. 4(a) and (b) shows the calculated T–HR–T curves obtained using the activation energies calculated by isoconversional method (solid lines) for both reactions. Fig. 4(c) and (d) shows the calculated T–T–T diagrams. In this case, the calculated curves were not compared with experimental data, because isothermal DSC experiments were not employed in this work.

#### 4. Discussion

The activation energy for the first transformation reaction ( $\text{Mg}_{50}\text{Ni}_{50} \rightarrow \text{Mg}_2\text{Ni} + \text{remaining amorphous}$ ) obtained by Kissinger method ( $135 \pm 4 \text{ kJ mol}^{-1}$ ) is similar to that obtained by isoconversional method ( $142 \pm 9 \text{ kJ mol}^{-1}$ ) within the limits of experimental errors. These values are lower than those reported by Orimo et al. [8] ( $210 \text{ kJ mol}^{-1}$ ) and Aydinbeyli et al. [15] ( $208\text{--}270 \text{ kJ mol}^{-1}$ ). On the other hand, as can be seen from Fig. 3(a), the value of this activation energy is practically constant with  $\alpha$ . Based on the results obtained, it is possible to conclude that the first transformation reaction is controlled by one reaction mechanism.

The activation energy for the second transformation reaction ( $\text{Mg}_2\text{Ni} + \text{remaining amorphous} \rightarrow \text{Mg}_2\text{Ni} + \text{MgNi}_2$ ) obtained by Kissinger method ( $200 \pm 2 \text{ kJ mol}^{-1}$ ) is within the range of the reported values [8,13] ( $198\text{--}408 \text{ kJ mol}^{-1}$ ), and is lower than the initial activation energy obtained by isoconversional method ( $170 \pm 5 \text{ kJ mol}^{-1}$ ). The variation of the activation energy with  $\alpha$  observed in Fig. 3(b) suggest that the second transformation reaction would be controlled by at least two reaction mechanisms, with activation energies of  $170 \pm 5 \text{ kJ mol}^{-1}$  and  $111 \pm 9 \text{ kJ mol}^{-1}$ , separated by a transition zone.

To determine the applicability of nucleation-growth model to the thermal transformation of  $\text{Mg}_{50}\text{Ni}_{50}$  into  $\text{Mg}_2\text{Ni}$  and  $\text{MgNi}_2$ , the testing method proposed by Málek [17,18] was employed. Based on the results obtained ( $\alpha_{\text{Mg}_2\text{Ni reaction}}^\infty = 0.49 \pm 0.03$  and  $\alpha_{\text{MgNi}_2\text{ reaction}}^\infty = 0.49 \pm 0.06$ ), which are far lower than the characteristic value ‘finger-print’ of nucleation-growth model ( $\alpha_\infty \approx 0.63 \pm 0.02$ ), it was determined that the Johnson–Mehl–Avrami nucleation-growth model could not be used to describe the kinetics of both reactions. This result can be related to the nanocrystalline–amorphous condition of the milled powders (Fig. 1), which can cause the overlap of grain growth and nucleation processes.

Download English Version:

<https://daneshyari.com/en/article/1483780>

Download Persian Version:

<https://daneshyari.com/article/1483780>

[Daneshyari.com](https://daneshyari.com)